A Journal of the Gesellschaft Deutscher Chemiker

Angewandte International Edition

GDCh

Chemie

www.angewandte.org

Accepted Article

Title: Chemical Cutting of Perovskite Nanowires into Single-Photon Emissive Low-aspect Ratio CsPbX3 (X= Cl, Br & I) Nanorods

Authors: Lakshminarayana Polavarapu, Yu Tong, Ming Fu, Eva Bladt, He Huang, Alexander F. Richter, Kun Wang, Peter Müller-Buschbaum, Sara Bals, Philippe Tamarat, Brahim Lounis, and Jochen Feldmann

To be cited as: *Angew. Chem. Int. Ed.* 10.1002/anie.201810110
Angew. Chem. 10.1002/ange.201810110

Link to VoR: http://dx.doi.org/10.1002/anie.201810110
http://dx.doi.org/10.1002/ange.201810110

WILEY-VCH

10.1002/anie.201810110

WILEY-VCH

COMMUNICATION

Chemical Cutting of Perovskite Nanowires into Single-Photon Emissive Low-aspect Ratio $CsPbX_3$ (X= Cl, Br & I) Nanorods

Yu Tong, Ming Fu, Eva Bladt, He Huang, Alexander F. Richter, Kun Wang, Peter Müller-Buschbaum, Sara Bals, Philippe Tamarat, Brahim Lounis, Jochen Feldmann, Lakshminarayana Polavarapu*

Dedication ((optional))

Abstract: *Post-synthetic shape-transformation processes provide access to colloidal nanocrystal morphologies that are unattainable by direct synthetic routes. Herein, we report our finding about the ligand-induced fragmentation of $CsPbBr_3$ perovskite nanowires (NWs) into low aspect-ratio $CsPbX_3$ (X=Cl, Br and I) nanorods (NRs) during halide ion exchange reaction with PbX_2-ligand solution. The shape transformation of NWs-to-NRs resulted in an increase of photoluminescence efficiency owing to a decrease of nonradiative decay rates. Importantly, we found that the perovskite NRs exhibit single photon emission as revealed by photon antibunching measurements, while it is not detected in parent NWs. This work not only reports on the quantum light emission of low aspect ratio perovskite NRs, but also expands our current understanding of shape-dependent optical properties of perovskite nanocrystals.*

Over the last few years, colloidal halide perovskite nanocrystals (NCs) have received significant interest owing to their extraordinary optical properties such as near-unity photoluminescence quantum yields (PLQYs), strong quantum confinement effects and quantum light emission.[1] These unique properties make them stand out in the forefront of many potential semiconductor materials for light emitting and photovoltaic applications.[2] The optical properties of perovskite NCs are tunable either by halide composition or through morphology control.[2a, 3] Despite recent success in the shape-control of perovskite NCs, currently, unlike for conventional semiconductor and metal NCs, we have access only to a limited number of perovskite nanostructures such as nanocubes, Nanoplatelets, nanosheets and NWs.[3-4] Whereas in the case of metal and conventional semiconductors, a myriad of nanostructure morphologies have been achieved.[5] Among all, colloidal NRs played an indispensable role in various applications of nanotechnology.[5] However, this striking morphology has been rarely achieved in the field of colloidal perovskite NCs.[6] Previous studies clearly suggest that it is challenging to stop the growth of all-inorganic perovskite NWs at the early stages of their growth in order to obtain NRs,[3, 7] which makes it difficult to prepare low-aspect ratio NRs by direct synthetic approach. Essentially, post-synthetic chemical and shape transformation processes offer accessibility to morphologies and chemical compositions that are difficult to synthesize by direct methods.[5, 8] These processes are also gaining attention in the field of perovskite NCs due to the fact that perovskites are soft in nature.[9] For instance, we have previously shown the ligand-induced transition from bulk hybrid perovskites to colloidal nanoplatelets of tunable thicknesses.[9a, 9e]

In this work, we report the shape-transformation of $CsPbBr_3$ perovskite NWs into a nearly-monodisperse low aspect ratio $CsPbX_3$ NRs during the ion exchange reaction (Figure 1). The colloidal dispersion of $CsPbBr_3$ perovskite NWs were prepared by the polar solvent-free, one-pot ultrasonication approach reported by our group.[3] The length of the as-prepared $CsPbBr_3$ NWs ranges from 1-2 μm with a uniform width of ~12nm (Figure 2a) and they exhibit green emission under UV light illumination. The $CsPbBr_3$ NWs exhibit relatively low PLQY (<10%), which was previously attributed to the presence of defects. To tune the emission color of NWs, we implemented well known halide ion exchange reaction between colloidal solution of $CsPbBr_3$ NWs and PbI_2-ligand complex in toluene.[3, 10] The complete halide ion exchange of Br with I in the NWs resulted in a well dispersed

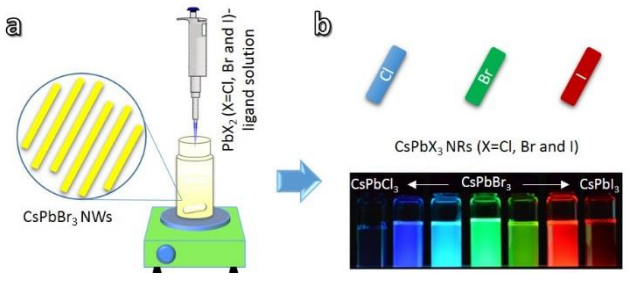

Figure 1. a) Schematic illustration showing the transformation of $CsPbBr_3$ perovskite NWs into $CsPbX_3$ NRs by the addition of PbX_2-ligand solution. b) Photograph of the colloidal dispersions of $CsPbX_3$ NRs with different halide (X=Cl, Br, and I) compositions under UV light (λ=367 nm) illumination.

[a] Y. Tong, Dr. H. Huang, A. F. Richter, Prof. Dr. J. Feldmann and Dr. L. Polavarapu
Chair for Photonics and Optoelectronics
Department of Physics and Center for NanoScience (CeNS),
Ludwig-Maximilians-Universität München
Amalienstr.54, 80799, Munich, Germany
Email: l.polavarapu@lmu.de

[b] Dr. M. Fu, Prof. Dr. Philippe Tamarat, Prof. Dr. B. Lounis
LP2N, Université de Bordeaux, Talence F-33405, France
LP2N, Institut d'Optique and CNRS, Talence F-33405, France

[c] Dr. E. Bladt, Prof. Dr. S. Bals
EMAT, University of Antwerp
Groenenborgerlaan 171, B-2020 Antwerp, Belgium

[d] K. Wang, Prof. Dr. P. Müller-Buschbaum
Technische Universität München, Physik-Department, Lehrstuhl für Funktionelle Materialien, James-Franck-Str. 1, 85748 Garching, Germany

Supporting information and the ORCID identification number(s) for the author(s) of this article can be found under:

10.1002/anie.201810110

WILEY-VCH

COMMUNICATION

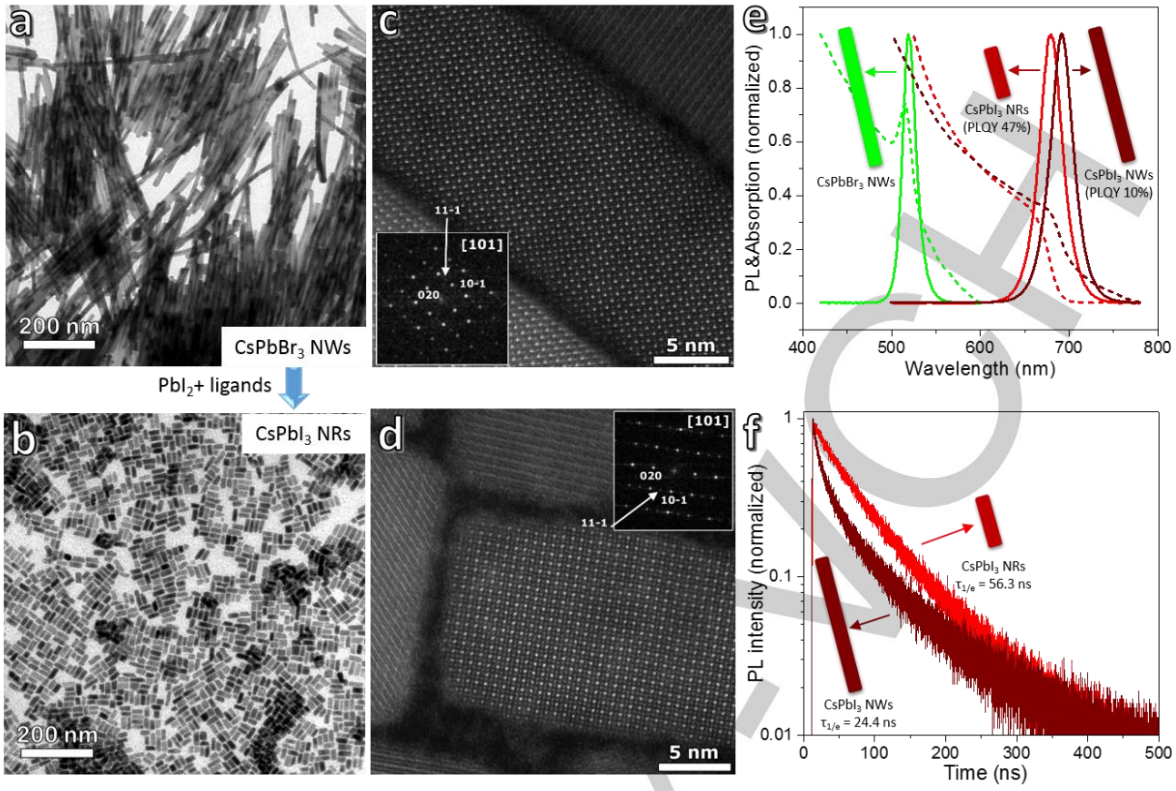

Figure 2. Bright-field TEM (a, b) and HAADF-STEM (c, d) images of parent $CsPbBr_3$ NWs and the $CsPbI_3$ NRs obtained after the halide ion exchange reaction with PbI_2-ligand solution. The diffractograms shown in the insets of figures c & d indicate that the $CsPbBr_3$ NWs and $CsPbI_3$ NRs have an orthorhombic crystal structure. (e) UV-vis extinction and PL spectra of $CsPbBr_3$ NWs, $CsPbI_3$ NWs and $CsPbBr_3$ NRs. (f) PL decay dynamics of $CsPbI_3$ NWs and NRs.

colloidal solution with bright red luminescence under UV lamp. In addition, weekly luminescent precipitate can be seen at the bottom of the glass bottle (Figure S1). The change in the PL emission color of NCs from green to red with a PL peak of the resultant NCs at ~680 nm indicates the nearly-complete exchange of Br with I (Figure 2e, S2). Such halide ion exchange generally preserves the morphology of the parent perovskite NCs.[6, 10] To our surprise, TEM images of the resultant red luminescent colloidal dispersion revealed that the $CsPbBr_3$ perovskite NWs fragment into low aspect-ratio $CsPbI_3$ NRs during the halide ion exchange process (Figure 2a, b). The corresponding bright-field TEM images of the supernatant show the presence of uniform $CsPbI_3$ NRs with an aspect-ratio mainly ranging from 2.5-3.5 (Figure 2b, S1), whereas the sediment consists of $CsPbI_3$ NWs with preserved morphology of $CsPbBr_3$ NW templates (Figure S1). It was staggering to see such low aspect ratio perovskite NRs due to the fact that it is difficult to obtain them by direct colloidal synthesis. The high-resolution high-angle annular dark field scanning TEM (HAADF-STEM) images of single NCs and corresponding diffractograms revealed that the orthorhombic crystal structure of the $CsPbBr_3$ NWs retains after the shape transformation into $CsPbI_3$ NRs (Figures 2c, d). The HAADF-STEM images of multiple $CsPbI_3$ NRs further confirm the high quality single crystalline nature of $CsPbI_3$ NRs (Figure S3). These perovskite NRs tend to self- assemble into ordered domains on silicon substrate as revealed by SEM characterization (Figure S4).

The $CsPbI_3$ NRs exhibit slightly blue-shifted extinction and photoluminescence compared to that of NWs due to quantum confinement caused by their decrease in length (Figure 2e). In addition, the PLQY of the $CsPbI_3$ NRs were found to be significantly enhanced from ~10% ($CsPbBr_3$ NWs) to ~47% ($CsPbI_3$ NRs) after the shape transformation. There are two main possible reasons for the enhanced PLQY after halide ion exchange. First, the ligands present in the PbI_2 precursor solution can passivate the surface trap states of NC, thus reducing nonradiative recombination channels. Second, the breakdown of NWs into NRs shortens the extent of exciton diffusion, thereby reducing the probability to find a nonradiative trap. Among these two reasons, it is likely that the observed increase of PLQY is a consequence of change of morphology due to that fact that the $CsPbI_3$ NWs present in the sediment exhibit only 10% PLQY similar to the templated $CsPbBr_3$ NWs. Time resolved PL decay studies revealed that the $CsPbI_3$ NRs exhibit longer exciton lifetime than the NWs due to reduced nonradiative decay rates (Figure 2f). These results suggest that the part of a NW having traps gets separated from the non-defective parts when the NW breaks into NRs, otherwise the excitons are likely to find a trap owing to large exciton diffusion lengths of perovskites. These features are exactly the opposite effects observed in the transformation of nanocubes to NWs through oriented attachment.[3] However, the PLQY of $CsPbI_3$ NRs is not as high as it was reported for corresponding nanocubes,[4c] which confirm that some of these NRs must still possess defect sites that can act as nonradiative channels. Temperature-dependent PL measurements revealed that the PLQY of $CsPbI_3$ NRs increases up to 90% at cryogenic temperatures (Figure S5). We attribute this to a decrease of the nonradiative decay rate, but we can also expect that there is an increase in the radiative decay of free excitons.[11]

10.1002/anie.201810110

WILEY-VCH

COMMUNICATION

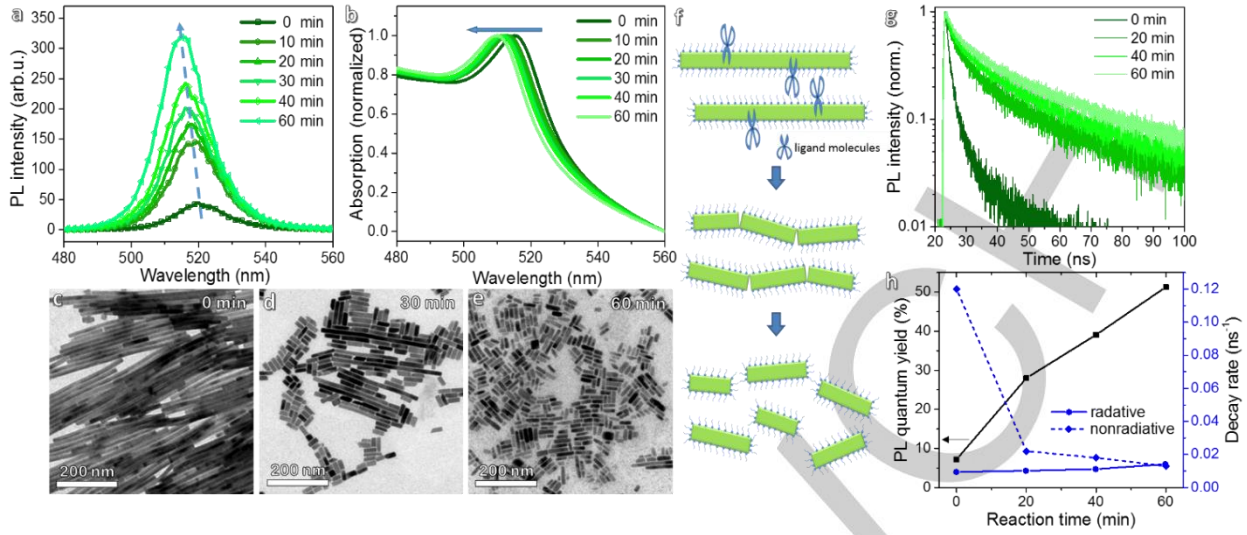

Figure 3. PL (a), UV-vis extinction (b) of colloidal $CsPbBr_3$ NCs obtained by the reaction of $CsPbBr_3$ NWs with oleylamine for different periods of time. (c-e) Corresponding TEM images. (f) Scheme showing the ligand-induced breakdown of NWs into NRs. (g) Corresponding PL decay dynamics and (h) plot depicting the PLQY, radiative and nonradiative decay of the obtained CsPbBr3 NCs as a function of reaction time.

Interestingly, similar shape transformations were observed by the reaction of $CsPbBr_3$ NWs with $PbCl_2$ and $PbBr_2$ precursor solutions, as illustrated in figure 1. The composition of the resultant $CsPbX_3$ NRs and thus their emission color is tunable by varying the amount of PbX_2 (X= Cl, Br and I)-ligand solution used for the ion exchange reaction (Figure S2). The optical bandgap of $CsPbX_3$ perovskite NRs is also tunable across the full visible wavelength range of 400-700 nm and the PL decay becomes slower while going from chloride to iodide via bromide (Figure S6). The corresponding X-ray diffraction patterns (Figure S7) as well as HAADF-STEM images (Figure 2d, S8) indicate that the $CsPbX_3$ NRs exhibit either cubic or orthorhombic crystal structures, while the HAADF-STEM analysis of $CsPbBr_3$ NWs suggest that they exhibit orthorhombic phase only (Figure 2c).[3] Despite interesting shape transformation from NW to NR, the mechanism of this process is still unclear. One possible reason could be the reduction of crystal lattice induced by the breakage of NWs into NRs. However, a quantitative analysis of the high resolution HAADF-STEM measurements images revealed that there is no significant trend in the interatomic distances of the nanocrystal lattices of before and after shape transformation (Figure S8), which rules out our hypothesis.

Such break down of NWs into NRs has some striking similarities with our previous findings on ligand-assisted fragmentation of bulk perovskites into perovskite nanoplatelets. [9a, 9e] Herein, we used the ligands oleylamine and oleic acid to dissolve the PbX_2 precursors in organic solvents. The excess ligands present in PbX_2 precursor solution can cause the fragmentation of NWs. Although the exact mechanism of this cutting process is unclear, it is likely that the ligands reacts with NWs randomly at different portions of the NWs, thus break them into NRs by particle dissolution at reaction sites. To test our assumption, a small volume of pure oleylamine (100 μL) was added to the colloidal solution of $CsPbBr_3$ NWs under continuous stirring and then the reaction was monitored by UV-vis extinction, PL, PL lifetime and correlative TEM characterization over a period of time (Figure 3). After 10 min, there is a steep increase in intensity and blue shift of PL peak and is then gradually increased in intensity with a continuous blue shift over the next 60 min (Figure 3a). Similarly, the UV-vis extinction spectra show a slight gradual blue shift with an increase in reaction time (Figure 3b). The corresponding TEM images acquired from the samples collected at different reaction time indicate that the blue shift of absorption and PL is caused by the change of morphology from NWs to NRs (Figure 3c-e). While the $CsPbBr_3$ samples exhibit high polydispersity, the average aspect ratio of the $CsPbBr_3$ NRs appears to be relatively decreased with increase of reaction time, thus resulting in a gradual blue shift of absorption and PL. While the PLQY increases significantly from 8-50%, the blue shift is small due to the fact that change of morphology is not leading to the size where the NCs exhibit strong quantum confinement. Time resolved PL measurements revealed that the PL lifetime gradually increases with decreasing average aspect ratio of NRs due to a significant decrease of nonradiative decay rate (Figure 3g). As discussed earlier, the separation of defect sites from the NWs during shape transformation can result in a significantly decrease of nonradiative channels, while the radiative decay rate increases slightly due to the decrease of size (Figure 3h). These results demonstrate that the shape transformation from NWs to NRs are most likely due to the presence of ligand molecules in the PbX_2-ligand solution as schematically shown in Figure 3f. Now, the question is whether the ligands induce melting or fragmentation of NWs in to NRs. The melting process can be ruled out based on the fact that there is no significant difference in the absorption intensity before and after the shape transformation. Therefore, the ligand molecule induces the fragmentation of NWs into NRs in a process similar to the fragmentation of 3D perovskites into 2D nanoplatelets due to their soft nature.[9a]

Recently, there has been a growing interest in exploring the perovskite NCs as single-photon source (quantum emitter), [12] which may have implications in quantum information technologies. To this end, we explored the quantum emitting properties of the prepared $CsPbX_3$ NRs in comparison with their NW counterparts. For single particle PL measurements, the colloidal NR solutions were first diluted in 1wt% poly(methyl methacrylate)/toluene solution and then spin-coated onto clean glass slides, as

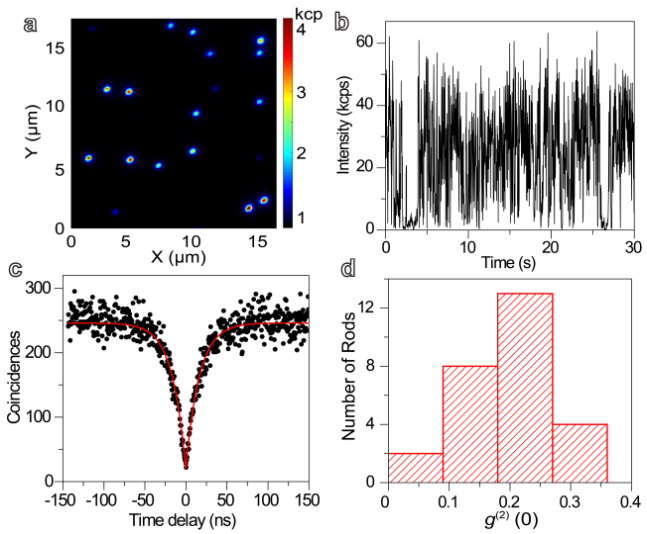

Figure 4. (a) Wide-field fluorescence image of $CsPbI_3$ rods dispersed in PMMA. (b) Time trace of the PL intensity of a single $CsPbI_3$ rod, recorded with a bin time of 20 ms under a CW excitation intensity of 100 W/cm^2. (c) Histogram of time delays between consecutive photon pairs detected from the fluorescence of a single $CsPbI_3$ rod, measured under a weak CW excitation intensity of 100 W/cm^2. The dip which approaches zero at zero time delay (with $g^{(2)}(0) \sim 0.1$), is a clear signature of photon antibunching. The single exponential fit (red solid line) corresponds to an exciton lifetime of 16 ns. (d) Distribution of $g^{(2)}(0)$ values.

described in the previous reports.[12d, 13] Figure 4a shows a wide-field fluorescence image of $CsPbI_3$ NRs which are well-separated from each other for single NR PL measurements. A representative time trace of PL intensity of single $CsPbI_3$ NR under continuous wave excitation at 488 nm is shown in figure 4b (see figure S9 for other examples). The PL of individual $CsPbI_3$ rods exhibits a characteristic blinking behavior, which is possibly due to the photoionization driven charging and discharging process, with a dominant Auger recombination in the decay of the charged excitons.[12a, 12b] While negligible in bulk semiconductors, the Auger effect is indeed strongly increased in quantum confined (QC) nanocrystals due to the enhanced Coulomb interaction between charge carriers and the reduced kinematic restriction on momentum conservation.[14] As the $CsPbI_3$ NRs are weekly QC, it is likely that the Auger processes can provide an efficient channel for exciton-exciton annihilation under intense laser excitation. This process drastically reduces radiative recombination of multiple excitons simultaneously created in the single NRs. Indeed, the PL intensity autocorrelation function $g^{(2)}(\tau)$ measured with a Hanbury Brown and Twiss setup under CW excitation reveals strong photon antibunching, which manifests as a dip of $g^{(2)}(\tau)$ at zero delay time (τ=0), as exemplified in Figure 4C (see other examples in Figure S9). We find $g^{(2)}(0) \sim 0.1$ (see Fig. 4d), close to the ideal signature $g^{(2)}(0) = 0$ of a pure single photon source. The main contribution to $g^{(2)}(0)$ is attributed to residual biexciton radiative recombinations. Fitting $g^{(2)}(\tau)$ with a single exponential rise function yields an exciton lifetime of 16 ns for this rod. Figure S10 displays a histogram of the lifetimes measured on various single rods, spread in the range 10-40 ns. With $g^{(2)}(0)$ values below 0.5 (Figure 4d), these single NRs may have potential use as quantum light sources. In contrast, the corresponding $CsPbI_3$ NWs neither show photon antibunching nor blinking characteristics (Figure S11). Although bundling of NWs cannot be completely ruled out, these results suggest that under intense laser excitation, multiple excitons can coexist at emission sites distributed all along a same NW and that their simultaneous radiative recombination is not efficiently quenched by Auger processes, and thus it is difficult to find only a single emitting event at any given time. It is thus a remarkable property that these NWs can be efficiently broken into low-aspect ratio NRs that exhibit quantum signatures in their emitted light. Furthermore, similar results were found from the single particle measurements of $CsPbBr_3$ NWs and NRs (Figure S12). It is worth mentioning that unlike nanocubes the anisotropic morphology of NRs may have additional benefits as single photon source.

In summary, we have presented the fragmentation of $CsPbBr_3$ NWs into nearly-monodisperse and low aspect ratio $CsPbX_3$ NRs of different halide compositions by halide ion exchange reaction. Through control experiments, we revealed that the ligands present in the precursor solution drive this process. This shape transformation leads to an increase of PLQY while retaining anisotropic morphology. The increase of PL efficiency is likely due to the removal of nonradiative trap sites from NWs by their fragmentation into NRs. Importantly, we have shown that these single NRs can serve as quantum light sources at room temperature. This work not only opens a door to access the morphologies such as NRs through post-synthetic shape transformations but also expands our current understanding of shape-dependent optical properties.

Acknowledgements

This work was supported by the Bavarian State Ministry of Science, Research, and Arts through the grant “Solar Technologies go Hybrid (SolTech)”, by the China Scholarship Council (Y.T. and K.W.), by the Horizon 2020 research and innovation program under the Marie Skłodowska-Curie Grant Agreement COMPASS No. 691185 and by LMU Munich’s Institutional Strategy LMU excellent (L.P., J.F.). M.F., P. T. and B. L. acknowledge the financial support from the French National Agency for Research, the French Excellence Initiative (Idex Bordeaux, LAPHIA Program) and the Institut Universitaire de France. E.B. and S.B. acknowledge the financial support from the European Research Council Starting Grant #335078-COLOURATOMS. L.P thank the EU Infrastructure Project EUSMI (European Union’s Horizon 2020, grant No 731019).

Keywords: $CsPbX_3$ nanocrystals • perovskite nanowires • perovskite nanorods • chemical cutting • shape transformation• single-photon emission

[1] a) L. Protesescu, S. Yakunin, M. I. Bodnarchuk, F. Krieg, R. Caputo, C. H. Hendon, R. X. Yang, A. Walsh, M. V. Kovalenko, *Nano Lett.* **2015**, *15*, 3692-3696; b) A. Swarnkar, V. K. Ravi, A. Nag, *ACS Energy Lett.* **2017**, *2*, 1089-1098; c) L. C. Schmidt, A. Pertegás, S. González-Carrero, O. Malinkiewicz, S. Agouram, G. Mínguez Espallargas, H. J. Bolink, R. E. Galian, J. Pérez-Prieto, *J. Am. Chem. Soc.* **2014**, *136*, 850-853.

[2] a) L. Polavarapu, B. Nickel, J. Feldmann, A. S. Urban, *Adv. Energy Mater.* **2017**, *7*, 1700267; b) Q. Wang, Z. Jin, D. Chen, D. Bai, H. Bian, J. Sun, G. Zhu, G. Wang, S. Liu, *Adv. Energy Mater.* **2018**, *8*, 1800007.

[3] Y. Tong, B. J. Bohn, E. Bladt, K. Wang, P. Müller-Buschbaum, S. Bals, A. S. Urban, L. Polavarapu, J. Feldmann, *Angew. Chem. Int. Ed.* **2017**, *56*, 13887-13892.

[4] a) L. Liu, S. Huang, L. Pan, L.-J. Shi, B. Zou, L. Deng, H. Zhong, *Angew. Chem. Int. Ed.* **2017**, *56*, 1780-1783; b) A. Dutta, S. K. Dutta, S. Das Adhikari, N. Pradhan, *Angew. Chem. Int. Ed.* **2018**, *57*, 9083-9087; c) Y. Tong, E. Bladt, M. F. Ayggler, A. Manzi, K. Z. Milowska, V. A. Hintermayr, P. Docampo, S. Bals, A. S. Urban, L. Polavarapu, J. Feldmann, Angew. Chem. Int. Ed. 2016, 55, 13887-13892; d) J. Shamsi, Z. Dang, P.

Bianchini, C. Canale, F. Di Stasio, R. Brescia, M. Prato, L. Manna, *J. Am. Chem. Soc.* **2016**, *138*, 7240-7243.
[5] L. Polavarapu, S. Mourdikoudis, I. Pastoriza-Santos, J. Pérez-Juste, *CrystEngComm* **2015**, *17*, 3727-3762.
[6] S. Aharon, L. Etgar, *Nano Lett.* **2016**, *16*, 3230-3235.
[7] a) D. Zhang, S. W. Eaton, Y. Yu, L. Dou, P. Yang, *J. Am. Chem. Soc.* **2015**, *137*, 9230-9233; b) M. Chen, Y. Zou, L. Wu, Q. Pan, D. Yang, H. Hu, Y. Tan, Q. Zhong, Y. Xu, H. Liu, B. Sun, Q. Zhang, *Adv. Funct. Mater.* **2017**, *27,* 1701121; c) M. Imran, F. Di Stasio, Z. Dang, C. Canale, A. H. Khan, J. Shamsi, R. Brescia, M. Prato, L. Manna, *Chem. Mater.* **2016**, *28*, 6450-6454.
[8] Q. A. Akkerman, S. Park, E. Radicchi, F. Nunzi, E. Mosconi, F. De Angelis, R. Brescia, P. Rastogi, M. Prato, L. Manna, *Nano Lett.* **2017**, *17*, 1924-1930.
[9] a) Y. Tong, F. Ehrat, W. Vanderlinden, C. Cardenas-Daw, J. K. Stolarczyk, L. Polavarapu, A. S. Urban, *ACS Nano* **2016**, *10*, 10936-10944; b) Y. Wang, X. Li, S. Sreejith, F. Cao, Z. Wang, M. C. Stuparu, H. Zeng, H. Sun, *Adv. Mater.* **2016**, *28*, 10637-10643; c_ J. Shamsi, P. Rastogi, V. Caligiuri, A. L. Abdelhady, D. Spirito, L. Manna, R. Krahne, *ACS Nano* **2017**, *11*, 10206-10213; d) Z. Liu, Y. Bekenstein, X. Ye, S. C. Nguyen, J. Swabeck, D. Zhang, S.-T. Lee, P. Yang, W. Ma, A. P. Alivisatos, *J. Am. Chem. Soc.* **2017**, *139*, 5309-5312; e) V. A. Hintermayr, A. F. Richter, F. Ehrat, M. Döblinger, W. Vanderlinden, J. A. Sichert, Y. Tong, L. Polavarapu, J. Feldmann, A. S. Urban, *Adv. Mater.* **2016**, *28*, 9478-9485; f) Q. A. Akkerman, V. D'Innocenzo, S. Accornero, A. Scarpellini, A. Petrozza, M. Prato, L. Manna, *J. Am. Chem. Soc.* **2015**, *137*, 10276-10281.
[10] G. Nedelcu, L. Protesescu, S. Yakunin, M. I. Bodnarchuk, M. J. Grotevent, M. V. Kovalenko, *Nano Lett.* **2015**, *15*, 5635-5640.
[11] J. Feldmann, G. Peter, E. O. Göbel, P. Dawson, K. Moore, C. Foxon, R. J. Elliott, *Phys. Rev. Lett.* **1987**, *59*, 2337-2340.
[12] a) Y.-S. Park, S. Guo, N. S. Makarov, V. I. Klimov, *ACS Nano* **2015**, *9*, 10386-10393; b) G. Rainò, G. Nedelcu, L. Protesescu, M. I. Bodnarchuk, M. V. Kovalenko, R. F. Mahrt, T. Stöferle, *ACS Nano* **2016**, *10*, 2485-2490; c) A. Swarnkar, R. Chulliyil, V. K. Ravi, M. Irfanullah, A. Chowdhury, A. Nag, *Angew. Chem. Int. Ed.* **2015**, *54*, 15424-15428; d) M. Fu, P. Tamarat, J.-B. Trebbia, M. I. Bodnarchuk, M. V. Kovalenko, J. Even, B. Lounis, *Nat. Commun.* **2018**, *9*, 3318.
[13] M. Fu, P. Tamarat, H. Huang, J. Even, A. L. Rogach, B. Lounis, *Nano Lett.* **2017**, *17*, 2895-2901.
[14] V. I. Klimov, A. A. Mikhailovsky, S. Xu, A. Malko, J. A. Hollingsworth, C. A. Leatherdale, H.-J. Eisler, M. G. Bawendi, *Science* **2000**, *290*, 314-317.

10.1002/anie.201810110

WILEY-VCH

COMMUNICATION

Entry for the Table of Contents

COMMUNICATION

Single photon emissive perovskite nanorods (NRs): $CsPbBr_3$ perovskite nanowires (NWs) break into low aspect-ratio $CsPbX_3$ (X=Cl, Br and I) NRs of different halide compositions by reaction with PbX_2-ligand solution. These perovskite NRs can serve as quantum light sources at room temperature, while the corresponding NWs did not show photon antibunching characteristics.

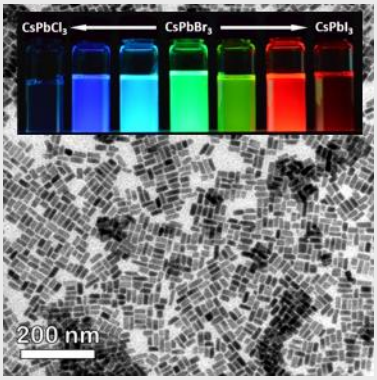

Y. Tong, M. Fu, E. Bladt, H. Huang, A. F. Richter, K. Wang, P. Müller-Buschbaum, S. Bals, P. Tamarat, B. Lounis, J. Feldmann, L. Polavarapu

Page No. – Page No.

Chemical Cutting of Perovskite Nanowires into Single-Photon Emissive Low-aspect Ratio $CsPbX_3$ (X= Cl, Br & I) Nanorods